Available online at www.sciencedirect.com
ScienceDirect
Journal of Molecular Graphics and Modelling 26 (2007) 760–774
Journal of Molecular Graphics and Modelling
www.elsevier.com/locate/JMGM

Exploring ligand recognition and ion flow in comparative models of the human GABA type A receptor

Younes Mokrab [a,1], Vassiliy N. Bavro [a,1], Kenji Mizuguchi [a,b,2], N.P. Todorov [c], Ian L. Martin [d], Susan M.J. Dunn [e], S.L. Chan [f], P.-L. Chau [g,*]

[a] *Department of Biochemistry, University of Cambridge, Cambridge CB2 1GA, United Kingdom*
[b] *Department of Applied Mathematics and Theoretical Physics, University of Cambridge, Cambridge CB3 0WA, United Kingdom*
[c] *De Novo Pharmaceuticals, Ltd., Compass House, Vision Park, Cambridge CB4 9ZR, United Kingdom*
[d] *School of Life and Health Sciences, Aston University, Birmingham B4 7ET, United Kingdom*
[e] *Department of Pharmacology, Faculty of Medicine and Dentistry, University of Alberta, Edmonton, Alberta T6G 2H7, Canada*
[f] *Chemical Computing Group, Inc., Suite 910, 1010 rue Sherbrooke Ouest, Montréal, Quebéc H3A 2R7, Canada*
[g] *Bioinformatique Structurale, CNRS URA 2185, Institut Pasteur, 75724 Paris, France*

Received 24 January 2007; accepted 29 April 2007
Available online 3 May 2007

Abstract

We present two comparative models of the $GABA_A$ receptor. Model 1 is based on the 4-Å resolution structure of the nicotinic acetylcholine receptor from *Torpedo marmorata* and represents the unliganded receptor. Two agonists, GABA and muscimol, two benzodiazepines, flunitrazepam and alprazolam, together with the general anaesthetic halothane, have been docked to this model. The ion flow is also explored in model 1 by evaluating the interaction energy of a chloride ion as it traverses the extracellular, transmembrane and intracellular domains of the protein. Model 2 differs from model 1 only in the extracellular domain and represents the liganded receptor. Comparison between the two models not only allows us to explore commonalities and differences with comparative models of the nicotinic acetylcholine receptor, but also suggests possible protein sub-domain interactions with the $GABA_A$ receptor not previously addressed.

Keywords: Ligand-gated ion channels (LGIC); $GABA_A$ receptor; GABA; Muscimol; Benzodiazepine; Flunitrazepam; Alprazolam; Halothane; Comparative modelling; Docking

1. Introduction

The family of γ-aminobutyric acid type A receptors ($GABA_A$ receptors) is responsible for the majority of fast neuronal inhibition in the mammalian central nervous system. These oligomeric proteins belong to the cys-loop family of ligand-gated ion channels that includes the nicotinic acetylcholine (nACh), glycine and $5HT_3$ receptors. The $GABA_A$ receptors are composed of five subunits arranged pseudosymmetrically around the integral anion channel [63]. The subunits, of which 19 have thus far been identified, are separated into classes based on their sequence similarity: there are six α-subunits, three β, three γ, three ρ and single representatives of δ, ε, θ and π. The precise subunit isoform composition of the oligomer defines the recognition and biophysical characteristics of the particular receptor subtype. The most ubiquitous subtype, which accounts for approximately 30% of $GABA_A$ receptors in the mammalian brain [95], contains two α_1-, two β_2- and a single γ_2-subunit [30].

The $GABA_A$ receptors can be divided into three structural domains. First, the large extracellular domain carries the recognition sites for both the natural agonist GABA and the clinically important benzodiazepines [3,27,96]. Secondly, the transmembrane domain forms the ion channel and contains the channel gate [4], in addition to an intra-helical hydrophobic pocket that is important for the interaction of these receptors with intravenous and volatile anaesthetics [39]. Finally, the intracellular domain contains portals through which ions access

* Corresponding author. Tel.: +33 145688546; fax: +33 145688719.
E-mail address: pc104@pasteur.fr (P.L. Chau).
[1] These authors contributed equally to this work.
[2] Present address: National Institute of Biomedical Innovation, 7-6-8 Saito Asagi, Ibaraki, Osaka 567-0085, Japan.

1093-3263/$ – see front matter
doi:10.1016/j.jmgm.2007.04.012

the cell cytoplasm. These portals appear to have a significant impact on channel conductance in other members of this family, i.e., the $5HT_3$ receptors [47] and the neuronal nAChRs [37].

The three-dimensional structure of the $GABA_A$ receptor has not yet been determined experimentally. A number of homology models have been constructed recently and these have been based on both the low resolution structure of the homologous *Torpedo* nAChR, obtained by cryoelectron microscopy [60,90] and the X-ray structures of related acetylcholine binding proteins (AChBP) [11,16–18,38], which are homologous to the extracellular domain of this receptor family. Here we have generated one such model using the most recently published structural information of the nAChR at 4 Å resolution [90]. This has allowed us to produce a homology model of the most common form of the $GABA_A$ receptor ($(\alpha_1)_2(\beta_2)_2\gamma_2$) that includes the extracellular, membrane-spanning and intracellular domains.

We have used this model (referred to here as model 1) to explore, for the first time, the ion passage through the complete receptor from the extracellular to the intracellular space. While recognising the restricted resolution of the side chains in several segments of the total structure, we have used this model to dock a number of ligands, having well-characterised recognition properties, to this particular $GABA_A$ receptor subtype. The recognition domains have been explored further by refining the docking results using either calculations of site electrostatic potentials or studies of the interactions of alternative conformers of the ligand that have known differences in their activity.

In addition, we have produced a second model (model 2) from more recently available data in which other homologous AChBPs have been crystallised in the presence of different ligands [16–18,38]. It is clear from these reports that the conformation of the receptor is distinct when occupied with agonist. Our data suggest that our model 1 is the apo-form of the receptor, while model 2 may represent an agonist-bound receptor complex that favours the open-channel conformation of the receptor. We have used model 2 to explore potential interactions that may occur only in the activated receptor.

Comparison of our models with hypotheses that have been developed for the nAChR in relation to the link between agonist recognition and channel gating [82,99] suggests that analogous interactions within the $GABA_A$ receptors are quite distinct. The purpose of this work has been to generate $GABA_A$ receptor models which can be tested experimentally and thus allow their further refinement.

2. Methods

2.1. Comparative modelling

The subunit composition we used for the $GABA_A$ receptor model has the stoichiometry $(\alpha_1)_2(\beta_2)_2\gamma_2$. This is the most common receptor subtype in the human central nervous system [5,70].

The amino acid sequences of the α_1- (P14867), β_2- (P47870) and γ_2- (P18507) subunits of the human $GABA_A$ receptor were taken from the UniProt [98]. A multiple alignment of these sequences, together with homologues collected by BLAST [1], was generated by MAFFT [46]. Putative transmembrane helices were predicted by THMHMM [49], which showed good agreement with the four conserved hydrophobic blocks in the alignment.

A structure-based alignment of all five chains of the nAChR structure [90] (PDB 2BG9) was generated with STAMP [73] and COMPARER [74]. Based on this alignment and the atomic coordinates, a structural profile for nAChR was created using FUGUE [78]. The multiple sequence alignment of the $GABA_A$ receptor was then aligned against this structural profile using FUGUE. The resulting sequence-structure alignment, annotated and examined with JOY [61], showed the four transmembrane helices (M1–M4) consistently aligned between nAChR and the $GABA_A$ receptor.

In the nAChR structure, most of the region between M3 and M4 appears to be disordered and no atomic coordinates are available, with the exception of the MA helices [90]. There is a long insertion of the $GABA_A$ receptor sequences corresponding to this region. This portion and the short N-terminal regions of the complete amino acid sequences (variable among the $GABA_A$ receptor subunits) were excised from the sequence-structure alignment. There was no obvious sequence conservation in the M3–M4 region and the alignment appeared to be ambiguous. Following the discussion by Ernst et al. [29], we have adopted their 'two-gap' alignment for this region, and the overall alignment was adjusted manually. Fig. 1 shows the final alignment of these sequences, and defines the amino acid numbering scheme we have used throughout this paper, the sequences being colour-coded according to [88].

For model building, only one template structure was chosen for each subunit of the $GABA_A$ receptor according to the following equivalences:

nAChR	$GABA_A$ receptor
α (2BG9 chain A)	β_2
β (2BG9 chain B)	γ_2
δ (2BG9 chain C)	α_1
α (2BG9 chain D)	β_2
γ (2BG9 chain E)	α_1

This equivalence is based on the position of the binding site for agonists. In the nAChR, the agonist binding site has the α-subunit on the C-loop side (by convention, the 'positive' side), and the δ- or γ-subunit on the F-loop side (the 'negative' side). In the $GABA_A$ receptor, the agonist activation site has the β-subunit on the 'positive' side, and the α-subunit on the 'negative' side.

These target-template pairs were extracted from the sequence-structure alignment and concatenated to create a single alignment corresponding to the entire receptor. This final alignment (see Fig. 1) was used as input to MODELLER [33,75] for building a model of the $GABA_A$ receptor. All five chains of the PDB entry 2BG9 were used simultaneously as the template. The modelled structure included the following residues:

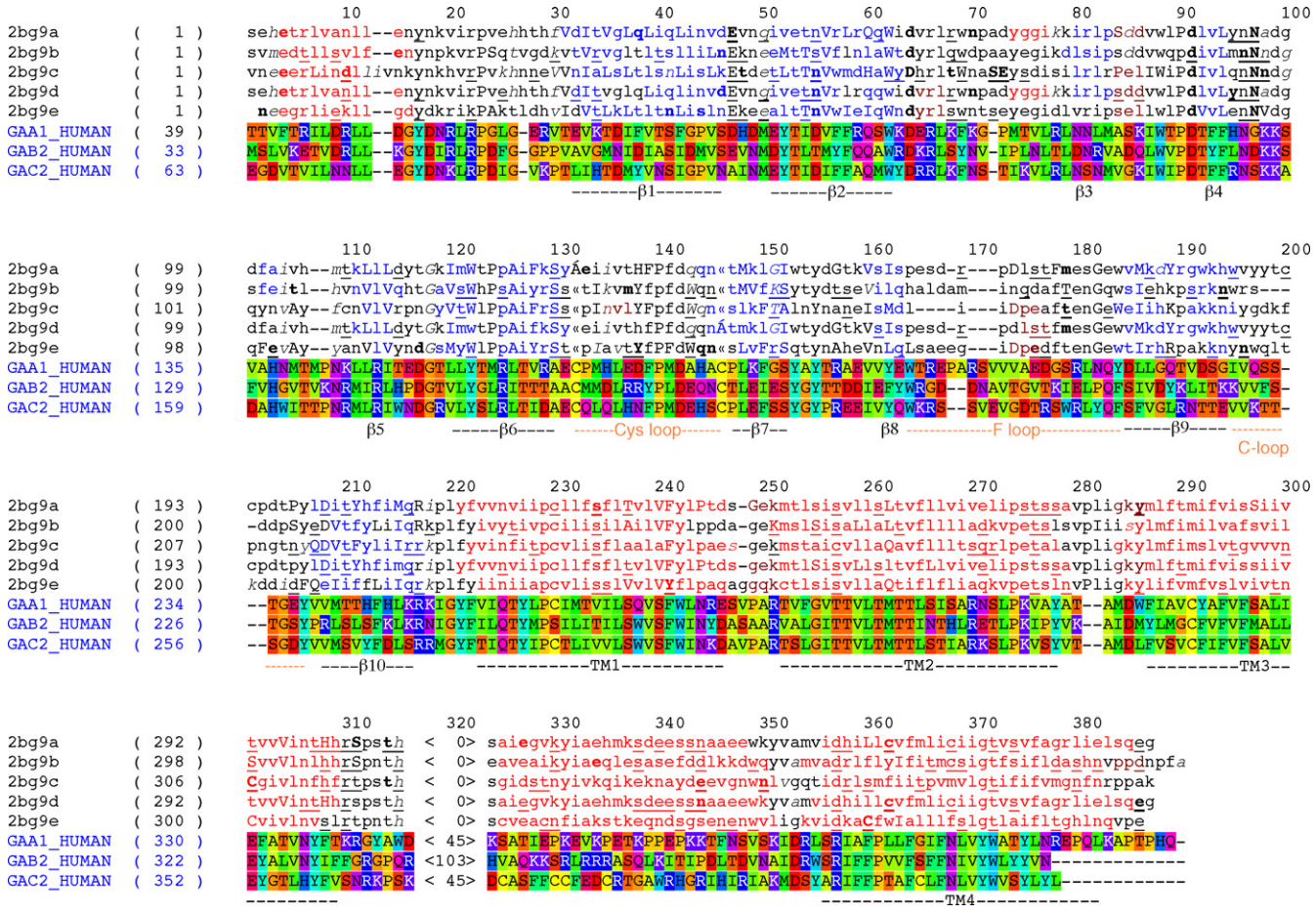

Fig. 1. Multiple structure-sequence alignment between the structures of the five subunits of the nicotinic acetylcholine receptor (nAChR) from *Torpedo marmorata* (PDB code: 2BG9) and the amino acid sequences of the α_1-, β_2- and γ_2-subunits of the human $GABA_A$ receptor. FUGUE [78] was used to align a combined structural profile involving the five chains of nAChR against the sequences of the $GABA_A$ receptor. Pair-wise alignments between corresponding subunits from the two receptors were then submitted to MODELLER: (1) nAChR chain A aligned against β_2 chain from human $GABA_A$ receptor (Swiss Prot P47870), (2) nAChR chain B against γ_2 chain from the human $GABA_A$ receptor (Swiss Prot P18507), (3) nAChR chain C against α_1 chain from the human $GABA_A$ receptor (Swiss Prot P14867), (4) nAChR chain D against β_2 chain from the human $GABA_A$ receptor, (5) nAChR chain E against α_1 chain from the human $GABA_A$ receptor. Membrane-spanning regions are underlined. Alignments were manually adjusted and formatted using JOY [61]. Insertions in the sequences of $GABA_A$ receptor chains were trimmed and numbers between brackets denote length of the insertions. The formatting convention of JOY is as follows: red, α-helices; blue, β-strands; maroon, 3_{10}-helices; upper case letters, solvent inaccessible; lower case letters, solvent accessible; bold type, hydrogen bonds to mainchain amides; underlining, hydrogen bonds to mainchain carbonyls; hydrogen bonds to other sidechain and/or heterogen groups; italic, positive mainchain torsion angles.

- β_2 (chain A) 33–337, 421–474;
- γ_2 (chain B) 63–367, 413–467;
- α_1 (chain C) 39–345, 391–456;
- β_2 (chain D) 33–337, 421–474;
- α_1 (chain E) 40–345, 391–456.

The model was examined using JOY [61] and its quality evaluated by Verify3D [56].

Using similar procedures, we built another model using the high-resolution structures of acetylcholine-binding protein (AChBP) from *Bulinus truncatus* [17], *Aplysia californica* [16] and *Lymnaea stagnalis* [18]. The Protein Databank entry codes for these three proteins are, respectively, 2BJ0, 2BR8 and 1UX2. The sequence alignment is shown in Fig. 2. We call this model 2.

A comparison of the two models were performed using the method MaxSub [80]. MaxSub performs a search for the largest subsets of C_α-atoms in each model, so would superimpose the structurally analogous atoms. This gives a more meaningful statistic for the difference between the two models.

2.2. Ligand docking

Coordinates for the GABA molecule were obtained from the PDB dataset 1QUR [87]. The Cambridge Structural Database was consulted for coordinates for muscimol (CSD code: MUSIMO01) [10], flunitrazepam (CSD code: CAGWUC) [15] and alprazolam (CSD code: CIZQAD01) [72]. The coordinates of halothane were generated *ab initio* and its geometry optimised according to the potential of Scharf and Laasonen [77]. These ligands were docked to model 1.

Ligand docking methods use search algorithms to rapidly explore the energy landscape of the protein-ligand interaction. To this end, two docking methods were used in this work, a genetic algorithm based method GOLD (version 2.0) [42,43,66], and easyDock, based on a novel

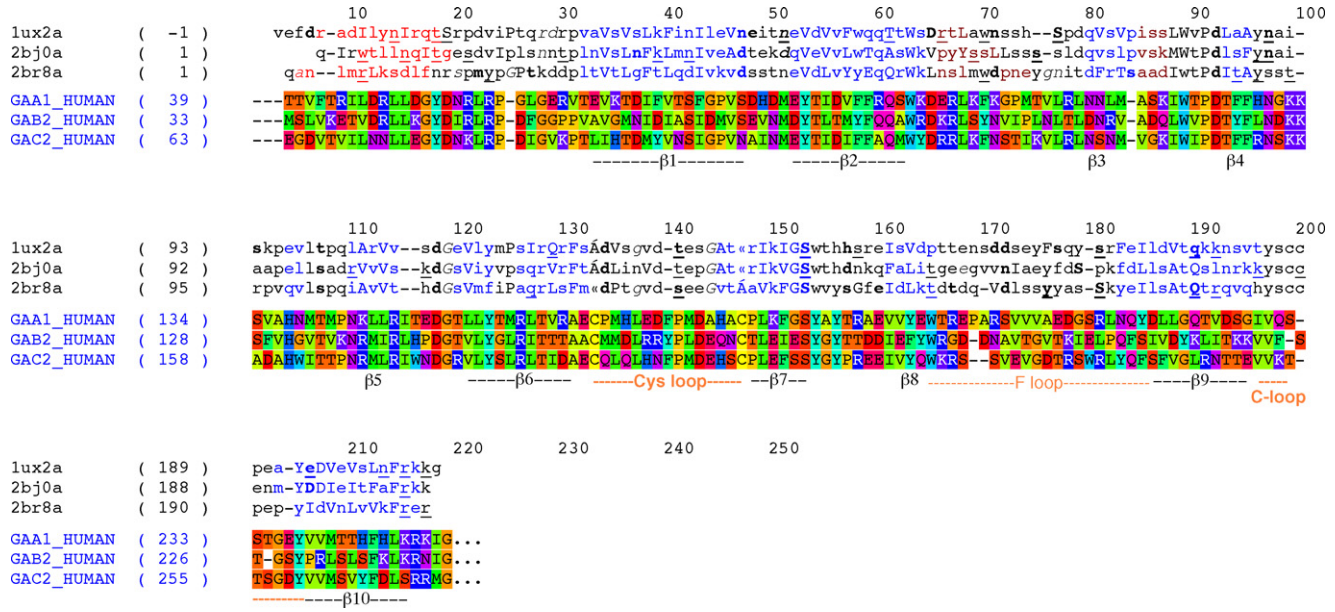

Fig. 2. Multiple alignment between the structures of acetylcholine binding proteins (AChBP) from *Lymnaea stagnalis* (1UX2), *Bulinus truncatus* (2BJ0), *Aplysia californica* (2BR8) and the amino acid sequence of the α_1-, β_2- and γ_2-subunits of the human $GABA_A$ receptor. The alignment was generated with FUGUE [78] and formatted with JOY [61]. The formatting convention of JOY is shown in the legend to Fig. 1.

optimization method called quantum stochastic tunnelling [44,57,89].

In stochastic tunnelling, 100 simulations were performed for each complex each consisting of 5×10^5 Monte Carlo steps. Several binding modes were generated with each docking simulation, yielding a limited number of ligand-binding modes. Approximate functions for describing ligand-protein interactions have been extensively investigated. The performance of these functions is limited by the difficulties in accurately treating the effects of solvation and the entropic changes due to hydrophobic interactions [48].

An analysis of the ligand-binding modes was performed in the following manner. Binding modes were ordered according to their binding scores. Then, starting from the lowest-energy solution, the root mean square deviation (RMSD) of each pose with respect to all the previous lower-energy poses was computed. If the RMSD was higher than a given threshold (3 Å), then that pose was added to a list of distinct solutions. The result of this procedure was a list of distinct ligand-binding mode poses that had RMSDs between one another of more than the pre-defined threshold.

All docking solutions were assigned to the nearest distinct binding mode and the distinct binding modes were re-ranked according to the number of docking solutions they attract, or their occupancy. This ranking procedure relates to concepts from the energy landscape theory describing the ligand-protein interaction. Consequently, it is possible to assume that many random initial conformations of the native ligand regularly dock in the stable (and dominant) binding mode. Nevertheless, due to the frustrated nature of the energy landscape and the limited search, alternative binding modes will also be found. Therefore, it is reasonable to expect that the most occupied binding mode would correspond to the native binding mode as observed experimentally.

Subsequent selection of one or more ligand-binding modes from the list of distinct docking poses were carried out on the basis of previous experimental data, known binding mode of other ligands and the electrostatic potential complementarity between the ligand and the receptor [20–22,25].

2.3. Evaluating the interaction energy profile of chloride ion passage

The potential experienced by a chloride ion passing from the extracellular to the intracellelular space was explored using the Amber99 potential [71] and the molecular modelling package MOE [58]. In this calculation, the z-direction was defined to be along the central pore from the extracellular side to the intracellular side.

The position of the chloride ion was initially at the extracellular end of the protein, at its axis of symmetry. The position of the ion was advanced by steps of 1 Å, in the positive z-direction (towards the intracellular space). The path remains at the axis of symmetry of the protein until it reaches the intracellular end of the transmembrane domain. At this point, the path splits into five. Each one is a straight line pointing outwards, going through the widest part of the portal (see Figs. 3 and 15 for illustrations of the paths).

The energy of interaction between the ion and the protein were evalulated at 1 Å intervals, with a relative permittivity of 1. We chose not to use a continuum approach because the ion channel pore is too small; explicit water molecules should be used for a thorough analysis. Moreover, any ion permeation analysis should consider multiple conformations of the protein,

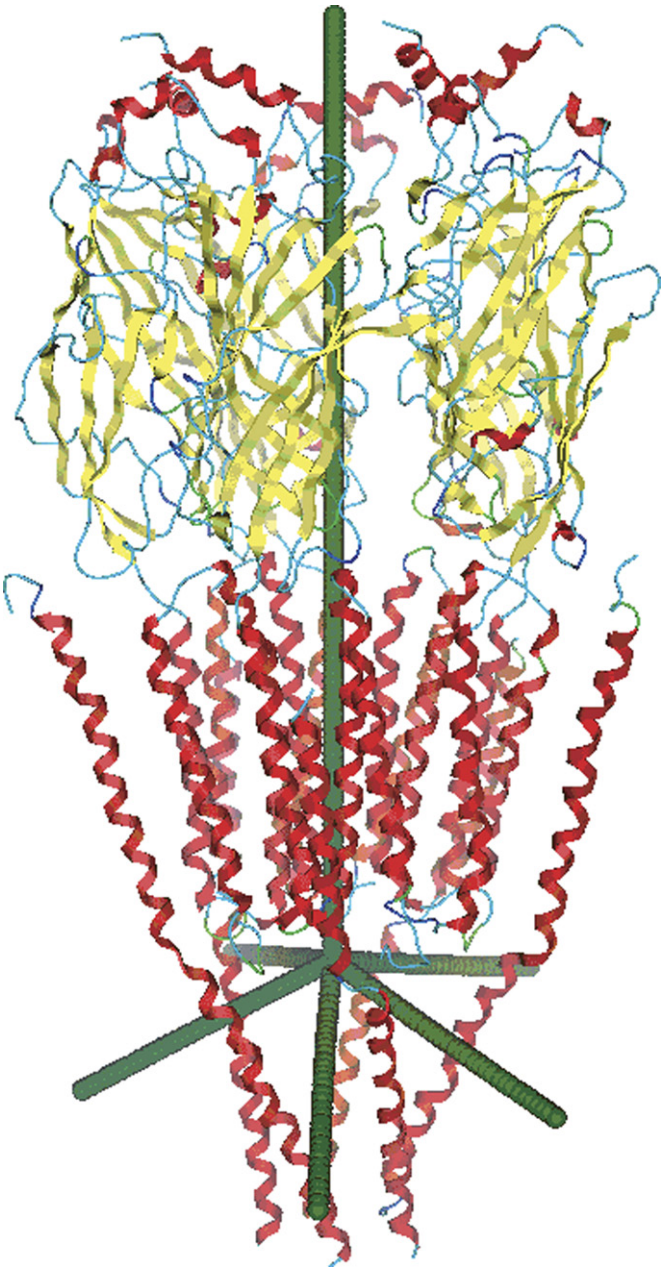

Fig. 3. Diagram showing the position of chloride ions, in the calculation of interaction energy between the Cl^- ion and the $GABA_A$ receptor model.

the water molecules and counter-ions, a significant task outside the focus of this work. This will be a complex project on its own. Here we only attempt to obtain an estimate of the potential along the path, so that we could validate our model by comparing our potential profile with the potential profiles obtained by other groups on other ion channel models.

3. Results

3.1. Structure of the two models

Model 1 is shown in Figs. 4 and 5. As it was based on the unliganded form of nAChR (2BG9), it is expected to present an apo-form. Since the majority of the templates for model 2 had

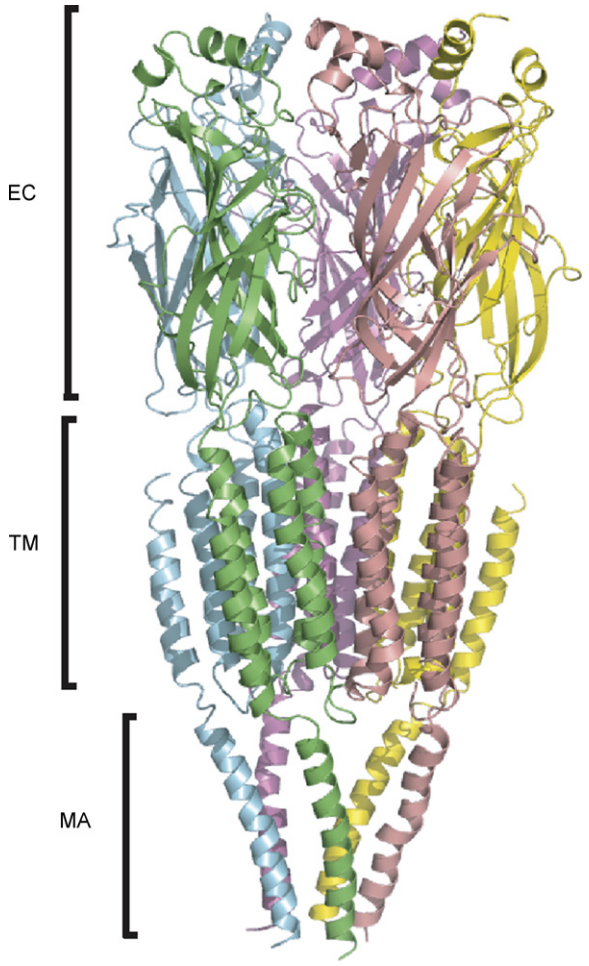

Fig. 4. Side view of model 1. The five subunits are shown in different colours. The extent of the extracelular domains are labelled EC, that of the transmembrane domains TM, and that of the helices of the intracellular domain are labelled MA. These helices are the only resolved structures in the nAChR, so we were only able to model this part of the intracellular domain.

the agonist binding sites occupied, they are expected to represent the agonist-bound form. For the different extracellular subunits, the MaxSub scores are follows:

Subunit	MaxSub score	Residues with RMS = 0
β_2 (chain A)	0.995	218/319 (56%)
γ_2 (chain B)	1.000	189/189 (100%)
α_1 (chain C)	0.986	210/213 (99%)
β_2 (chain D)	0.991	217/319 (68%)
α_1 (chain E)	0.991	210/212 (99%)

After we built our models, several new structures of AChBP were released [38]. They include structures with PDB codes 2BYN and 2BYQ. As expected, the comparison of model 1 with these newly solved structures shows that model 1 is indeed most closely related to the apo-structure of the AChBP (2BYN), while model 2 is virtually identical to the liganded conformation as presented by the structure 2BYQ [38]. Both models have a good overall fit when superimposed with any of the novel structures (overall RMSD from 1.3 to 1.4 Å), with most significant differences appearing in the region of the F-loop and especially the C-loop, where the RMSD approaches 10.5 Å (see

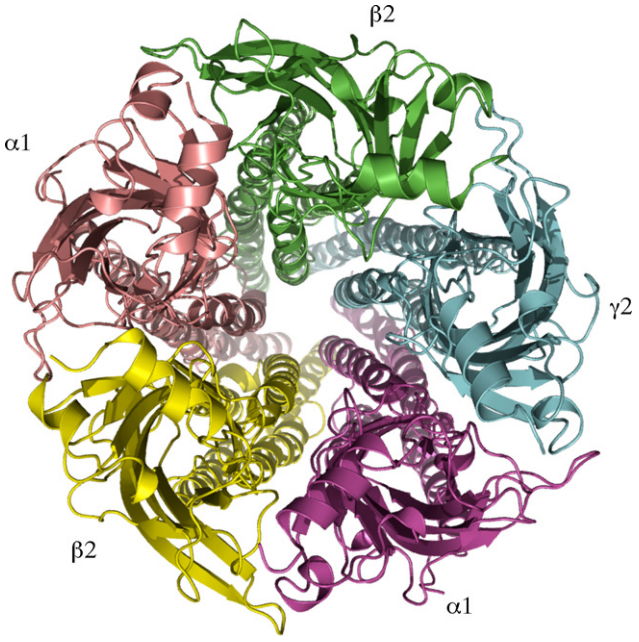

Fig. 5. View of model 1 from the extracellular space towards the intracellular space (the 'top' view). The five different subunits are labelled.

Fig. 6). Comparison of model 2 with 2BYQ, however, gives an RMSD over the C-loop region (<1.2 Å) which is lower than the overall C_α-backbone RMSD of about 1.35 Å, suggesting that it is an appropriate model of the agonist-bound form of the receptor. It should be noted, however, that both the C-loop and the F-loop are relatively non-conserved between AChBPs/AChR and GABA receptors, and as such are harder to model using comparative approaches.

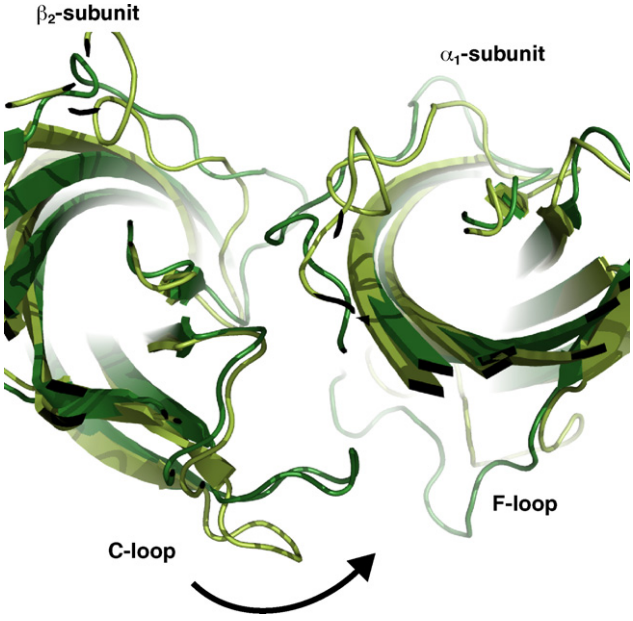

Fig. 6. A comparison of the binding-site region of models 1 and 2. The angle of view is from the extracellular space towards the intracellular space. Only the two subunits adjacent to the GABA-binding site is shown. Model 1 is shown in light green, while model 2 is shown in dark green. The arrowed line denotes the postulated direction of movement of the C-loop.

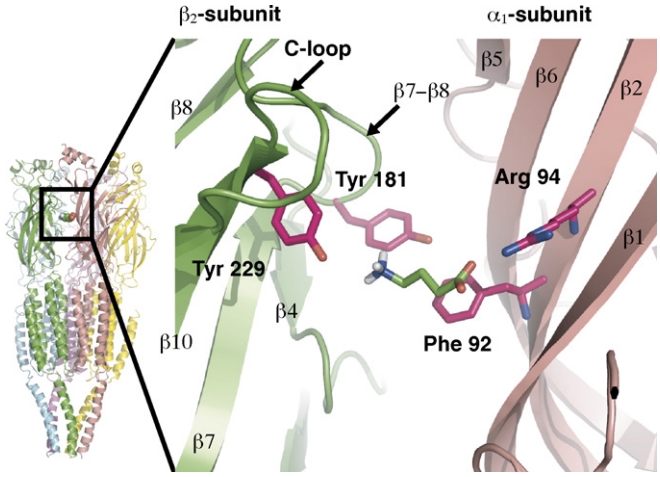

Fig. 7. Diagram showing the position of the GABA/muscimol-binding site and a docked GABA. The whole protein is shown on the left, and the area boxed in black, between two subunits, is the binding site for GABA and muscimol. The boxed region is enlarged to show GABA docked into the binding site of model 1. The protein main chains are colour-coded according to subunit, with four amino acids implicated in binding shown in magenta. The different β-strands and loop regions are annotated. Only one GABA configuration was found to be docked in this position, with the NH_4^+ of GABA facing Tyr 229.

3.2. Structure of the GABA-binding site

Fig. 7 shows the position of the GABA-binding site in the whole protein. The GABA activation sites are located between the β_2- and the α_1-subunits, so there are two GABA binding sites on each pentameric receptor. Experimental data have shown the following amino acids to be important for ligand recognition. On the α_1-subunit, these are Phe 92 [81,83], Arg 94, Ser 96 [9], Arg 147 [94] and Ile 148 [93]. On the β_2-subunit, they are Tyr 181, Thr 184 [3], Thr 226, Ser 228, Tyr 229, Arg 231 and Ser 233 [3,91].

3.3. Docking ligands to the GABA-binding site

Using the programme easyDock [89] and $GABA_A$ receptor model 1, we obtained 582 configurations for GABA docking and 633 configurations for the docking of muscimol.

A distance-screen was used to select GABA docked poses lying within 6 Å of four amino acids that have been experimentally identified as primary determinants for agonist recognition: Phe 92 [81,83] and Arg 94 [9] of the α_1-subunit, in addition to Tyr 181 and Tyr 229 of the β_2-subunit [3]. Six of 582 solutions fulfilled these criteria, five of which formed one cluster with a single outlier. The single outlier showed the charged amino group of GABA facing Tyr 229, with the carboxylate facing Arg94 (Fig. 7). In the high-population cluster, the charged amino group of GABA faces Phe 92, with the carboxylate positioned between Tyr 181 and Tyr 229 (Fig. 8).

In order to decide which binding mode is more probable, electrostatic potential complementarity was computed for the two binding modes. This is an empirical approach that has been developed to account for the interaction between charged ligands and their receptors [20–22,25] and is useful to predict the more likely docking configuration when there are

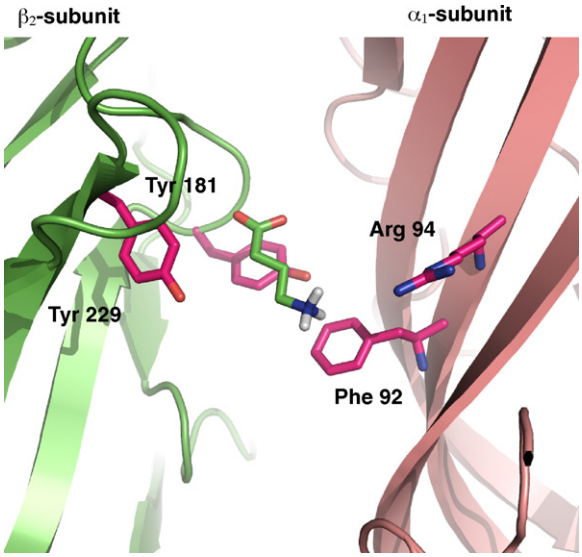

Fig. 8. View of GABA docked into the binding site of model 1. The view of this diagram is the same as Fig. 7. Five configurations were found to be docked in this position, with the carboxylate group of GABA facing Tyr 181 and Tyr 229. The protein main chains are colour-coded according to subunit, with four amino acids implicated in binding shown in magenta.

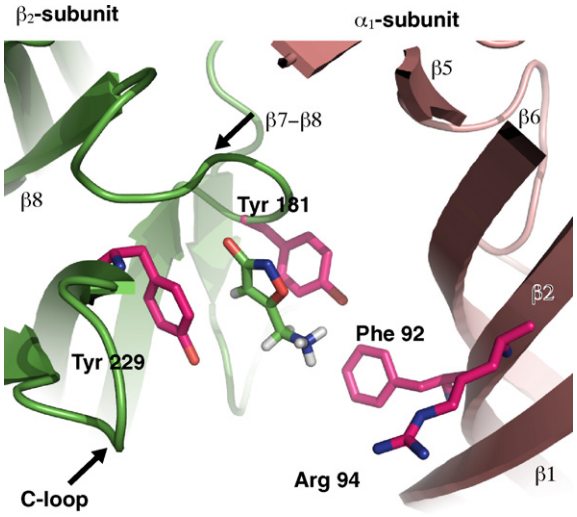

Fig. 9. View of muscimol docked into the binding site of model 1. The region of this diagram is the same as Fig. 7, but the angle of view is tilted in the extracellular direction by 15°. The protein main chains are colour-coded according to subunit, with four amino acids implicated in binding shown in magenta. The angle of view in this diagram is slightly different from that of the previous two diagrams, in order to display the oxazolo ring of muscimol more clearly.

insufficient experimental data to discriminate amongst multiple docked configurations.

In the cases of the two different docking configurations of GABA, charges were assigned to the ligand and receptor atoms using the Amber99 potential and the CHARMM potential [71]. A set of points on a sphere were produced by icosahedral tessellation [19]. These points were placed on the van der Waals sphere of each atom, and the interior points deleted to produce a set of points on the van der Waals surface of the molecule. The electrostatic potential at each van der Waals point due to the ligand, and that due to the protein, were evaluated. Spearman's rank correlation coefficient, r_s [85,86], was calculated for the two sets of electrostatic potentials to quantify the complementarity: at perfect complementarity, $r_s = -1$, but at perfect similarity, $r_s = 1$. This protocol is detailed in [20].

Using this analysis, for the high-population cluster of docked GABA (where its carboxylate tail is 'sandwiched' between Tyr 181 and Tyr 229), Spearman's rank correlation coefficient is −0.69 (Amber99 partial charges) or −0.65 (CHARMM partial charges). For the other configuration where the GABA NH_3^+-head faces Tyr 181 and Tyr 229, the rank correlation coefficient is −0.05 (both Amber99 and CHARMM partial charges). This analysis suggests that the former configuration (Fig. 8) is the more likely binding mode.

Using the same parameters for selection of the docked poses for muscimol, the highest scoring member has the oxazolo ring (carboxylate isostere) sandwiched between the faces of Tyr 181 and Tyr 229 and the charged amino terminus of muscimol appropriately positioned to delocalise to the π-cloud of Phe 92 (see Fig. 9). This particular orientation of muscimol is consistent with the suggestion by Amin and Weiss [3]; they noted in their mutagenesis study that Tyr 181 had an approximately three-fold greater effect on reducing the EC_{50} for muscimol activation compared to that of GABA. These authors suggested that as the primary structural difference between GABA and muscimol was the oxazolo ring, it was probably in close proximity to Tyr 181, thus supporting the orientation shown in Fig. 8.

A tryptophan residue occupies the equivalent position to Tyr 181 in the *Torpedo* nAChR α-subunits and the mouse $5HT_{3A}$ homomeric receptor. In both cases it has been shown that this residue exhibits cation-π delocalisation interactions with the charged amines of their natural agonists; estimates of interaction strength being 10 and 17 kJ/mol, respectively [6]. This orientation is not supported by the docked poses generated in this work for either muscimol or the high-population cluster for GABA. However, the single cluster outlier for GABA does adopt an orientation consistent with that found for both acetylcholine and 5HT [6], and it has been proposed that GABA adopts this orientation in the homomeric $GABA_C$ receptor [54]. In this orientation it would be possible for GABA carboxylate to form an ion-pair interaction with Arg 94.

Clearly the docked positions for GABA and muscimol are predicated upon the criteria used in their selection. The amino acids that we used here to guide our selection are found at the centre of a cluster of amino acids, mutation of which has been shown to compromise agonist recognition. It seems reasonable to suggest that the other amino acids, previously implicated in agonist-receptor interactions, may lie on the access or egress routes of the ligand as it approaches its docked site from either above (the most extracellular) or below (close to the membrane) the C-loop, which appears to close to envelop the ligand (see Fig. 6). Mutations of such residues are likely to affect the properties of agonist association or dissociation. Alternatively, other previously identified residues may be involved downstream

of the initial binding event, i.e., the agonist-induced conformational change that facilitates channel opening.

In the present study, we have identified a number of additional amino acids, lying within 6 Å of the docked ligand, that have not previously been explored. One of these, Phe73, decreases GABA potency by a factor of 20 when mutated to alanine [26]. Interestingly this amino acid is found about 5 Å from Phe 92 and the same distance from the amino terminus of GABA when it is docked in its preferred orientation. The two aromatic rings face the partially charged amine of GABA and Phe 73 is found close to the F-loop, the solvent accessibility of which has been shown to change on agonist activation ([64]; see Section 4).

3.4. Structure of the benzodiazepine-binding site

The left panel of Fig. 10 shows the position of the benzodiazepine-binding site in the whole protein. The benzodiazepine binding site lies between the α_1- and the γ_2-subunits, so there is only one such binding site on each pentameric receptor. Experimental data have shown the following amino acids to be important in benzodiazepine binding to the protein. On the α_1-subunit, these are His 129 [27,28,84,96], Tyr 187 [2], Gly 228 [76], Thr 234 and Tyr 237 [13]. On the γ_2-subunit, they are Met 96 [14,51], Tyr 97 [51], Phe 116 [12], Ala 118 [50] and Met 168 [51,97].

3.5. Docking ligands to the benzodiazepine binding site

Evidence that the α_1-subunit His 129 is an essential recognition site point for the benzodiazepines was based initially on mutagenic data [96]. However, it has subsequently been shown that photo-activation of flunitrazepam, bound to the benzodiazepine recognition site, results in the transfer of N1-methyl tritium to this amino acid [27]. The proximity of this

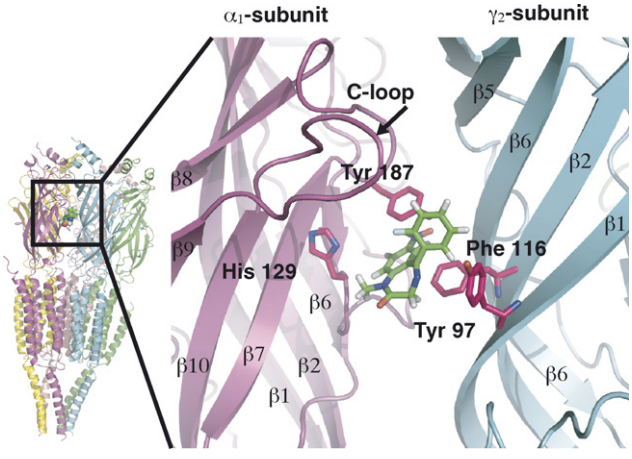

Fig. 10. Diagram showing the position of the benzodiazepine-binding site. The whole protein is shown on the left, and the area boxed in black, between two subunits, is the binding site for benzodiazepines. The boxed region is enlarged to show the active form of flunitrazepam docked into the binding site of model 1. The protein main chains are colour-coded according to subunit, with four amino acids implicated in binding shown in magenta. The different β-strands and loop regions are annotated.

histidine to the nitro-function of the benzodiazepine A-ring (the benzodiazepine ring fused to the seven-membered heterocycle) has recently been explored by the synthesis of a cysteine-reactive benzodiazepine, in which the nitro function at position 7 of the A-ring is replaced by isothiocyanate. Covalent modification of the mutant α_1-subunit His 129 Cys with this novel benzodiazepine [7] suggests that the 7-carbon of the A-ring is within 8.3 Å of the His 129 α-carbon. The mutation α_1-subunit Tyr 187 to Ser completely ablates benzodiazepine recognition suggesting that this is important in benzodiazepine binding [2]. There is significantly less information concerning residues within the γ_2 subunit involved in benzodiazepine recognition, although there is evidence that both the γ_2-subunit Tyr 97 [51] and the γ_2-subunit Phe 116 [12] are important site-points in ligand recognition. The docking solutions were subjected to a distance screen using these residues, employing similar criteria to those described for the GABA-docking above.

The seven-membered heterocycle of the benzodiazepines is thought to exist in two energetically distinct conformers. It has been suggested, as a result of the synthesis of conformationally restricted analogues, that the classical benzodiazepines have a preferred conformation for receptor interaction [8]. We have thus docked both alternative conformations to model 1, using the same docking paradigm, GOLD. An initial distance screen was used to explore the docked poses obtained, which were then clustered, as described previously. The preferred pose of the active conformer of flunitrazepam is shown in the right panel of Fig. 10. It places both the N1-methyl and the 7-nitro function in appropriate apposition to the α_1-subunit His 129, with the pendant 5-phenyl positioned between the α_1 Tyr 187 and the γ_2 Tyr 97 and the benzodiazepine A-ring about 3 Å from the γ_2 Phe 116 though not coplanar with it. It is interesting to compare this docked flunitrazepam position with early structure–activity models developed for the benzodiazepines (see [34]). Inspection of the docked position of the active flunitrazepam conformer suggests that 4′-phenyl substituents impact closely on γ_2 Phe 116, γ_2 Tyr 97 and γ_2 Asn 99. Finally, γ_2 Arg 183 is favourably located to act as a hydrogen bond donor to the heterocycle oxygen at position 2.

The orientation of the inactive conformer in the site is shown in Fig. 11. It is quite distinct from that described for the active conformer, but occupies essentially the same physical space. The α_1-subunit His 129 is equidistant from both the N1-methyl substituent of flunitrazepam and its A-ring nitro function, while α_1 Tyr 187 is within 3.5 Å of the benzodiazepine A-ring, although these rings are not parallel. The pendant C-ring of the benzodiazepine is almost coplanar with the γ_2 Phe 116 with the γ_2 Tyr 97 positioned to provide steric restriction to the site some 4.5 Å from the 4′ carbon of the C-ring, a substituent position known to be particularly sensitive to steric factors [34].

We also carried out a similar docking experiment with the imidazobenzodiazepine, alprazolam. The physical space occupied by this imidazobenzodiazepine is similar to that found for flunitrazepam but the orientation is distinct (Fig. 12). Alprazolam is an agonist benzodiazepine, like flunitrazepam, but has a significantly higher affinity for the recognition site. It is thus

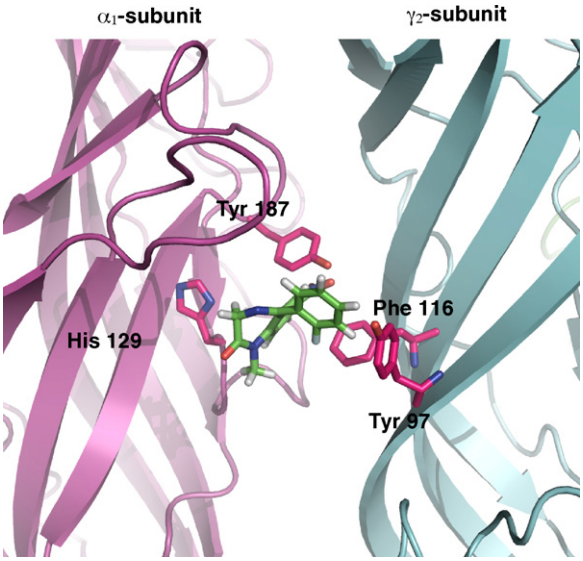

Fig. 11. View of the inactive form of flunitrazepam docked into the benzodiazepine binding site of model 1. The protein main chains are colour-coded according to subunit, with four amino acids implicated in binding shown in magenta.

interesting to note that the imidazo-ring on the *a*-face is found in closer proximity to the important recognition determinant α_1 His 129 than is the case with flunitrazepam, while the pendant phenyl sandwiched between the α_1 Tyr 187 and the γ_2 Phe 116 is within 3.5 Å of the A-ring of alprazolam, but not completely coplanar with it. It is possible that these favourable interactions may provide an explanation for the increased affinity of the interaction.

3.6. The halothane binding site

Previous work has identified three amino acids as important for general anaesthetic action: Leu 259, Ser 297 and Ala 318

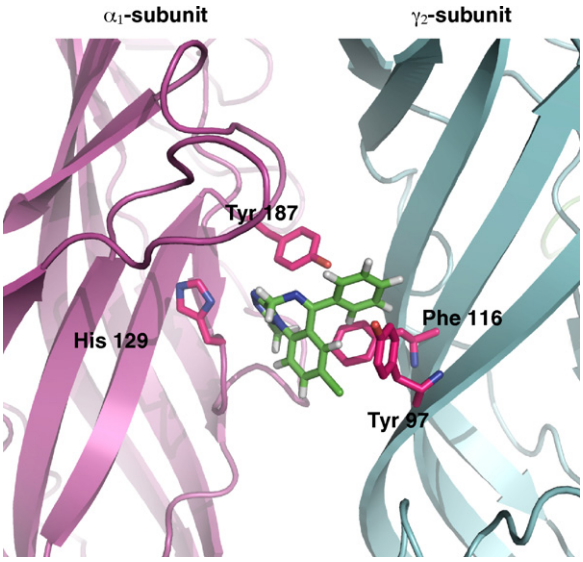

Fig. 12. View of alprazolam docked into the benzodiazepine binding site of model 1. The protein main chains are colour-coded according to subunit, with four amino acids implicated in binding shown in magenta.

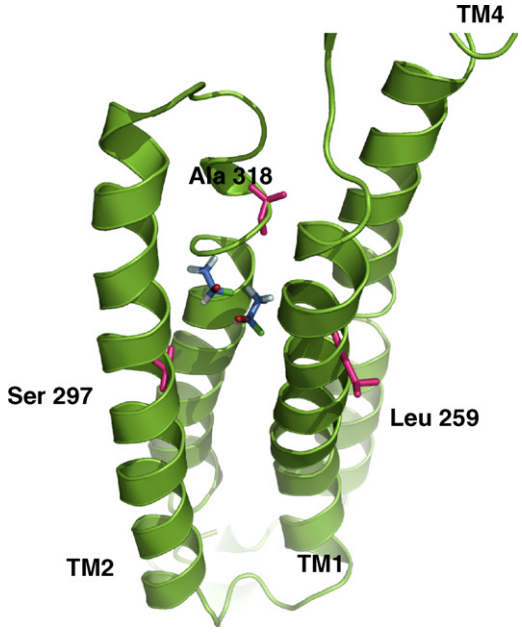

Fig. 13. View of halothane docked to its putative binding site of model 1, in the α_1-subunit. The carbon atoms of halothane are shown in blue, to distinguish them from the main chain ribbon. The protein main chains are shown in green, with the amino acids implicated in binding shown in magenta and labelled. They are Leu 259 of transmembrane domain 1 (TM1), Ser 297 of TM2 and Ala 318 of TM3.

[41]. Binding sites for the general anaesthetics have also been explored by homology modelling [100]. In this work, we docked halothane to this putative binding site on the α_1-subunit, and obtained three docked configurations. Two of them cluster together, but the third one is distinct. In Fig. 13, we show one member of the two-membered cluster, and the third binding configuration. It can be seen that the side chain of Leu 259 points away from the putative binding site; how this amino acid affects general anaesthetic action is still unclear. Ser 297 and Ala 318, on the other hand, point with their side chains towards the docked halothane structure. Indeed, the docked halothane appears to span the distance between these two amino acids. These results are consistent with those of Ernst et al. [29].

3.7. Ionic passage through the channel

We plot the interaction energy between a Cl^- ion and the modelled protein in Fig. 14. As described in the methods section, the interaction energy was calculated along the central pore of the extracellular and the transmembrane domains as well as along exit paths in the intracellular domain through each of the five portals (see Fig. 3). In Fig. 14, we show the interaction energy profile for the passage of a chloride ion. The profile through the five portals are coded in different colours, and their positions with respect to the protein are shown in Fig. 15.

Along the whole passage, electrostatic energy dominates over van der Waals energy. The interaction for the ion is generally favourable inside the protein.

When the Cl^- ion is at the extracellular end of the receptor, the interaction energy between the ion and the protein is about

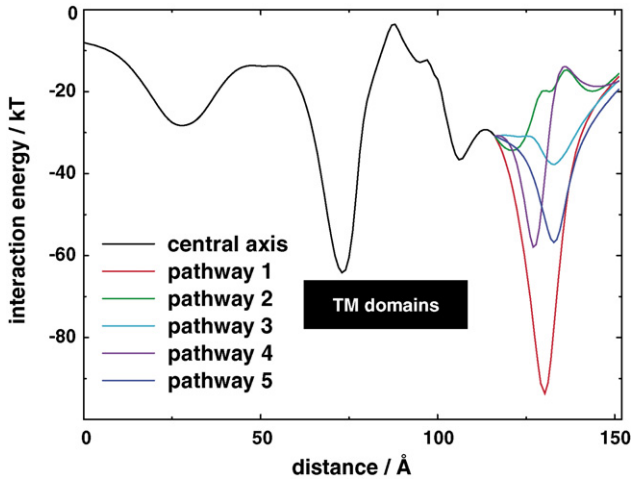

Fig. 14. Diagram showing the interaction energy between the protein and a Cl^- ion as it travels along the ion channel pathway. At distance = 0 Å, the chloride ion is at the extracellular end of the receptor. The position of the transmembrane domains is marked by a black bar. The interaction energy is calculated along the axis of symmetry until the ion reaches the boundary of the transmembrane and intracellular domains, distance = 116 Å. From this point the interaction energy is calculated along five paths which extend laterally from the axis of symmetry to pass through the widest part of the portals, formed between the intracellular MA helices and the intracellular face of the transmembrane domain. The energy profile of five different pathways through the five different portals are shown in different colours.

zero. As the ion enters, the energy decreases. The shallow trough about 30 Å from the extracellular end is mostly due to two nearby lysines, Lys 136 of the β_2-subunits. The interaction energy increases slightly, and then reaches a much lower minimum about 75 Å from the extracellular entrance. There are six lysines nearby, namely Lys 298 of the β_2-subunits, Lys 306

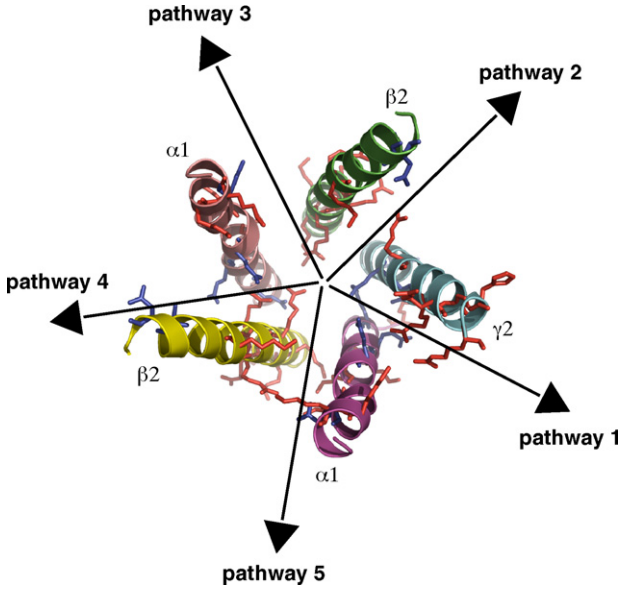

Fig. 15. Diagram showing the modelled structure of the intracellular helices. The angle of view is from the extracellular side towards the intracellular side, with the line of sight parallel to the ion channel axis. The positively charged amino acids are shown in red, while the negatively charged ones are shown in blue. The black arrow shows the approximate direction through which the chloride ion exits the ion channel.

of the α_1-subunits, and Lys 324 and Lys 328 of the γ_2-subunit. This is near the junction of the extracellular and transmembrane domains. The interaction then increases around the narrow region of the transmembrane domains, with the presence of the β_2-subunit Thr 284, Thr 287 and His 291, the α_1-subunit Thr 292, Thr 295 and Ile 298, and the γ_2-subunit Leu 313, Thr 317 and Ile 321. At the intracellular end of the central pore, near the interface of the transmembrane domain and the intracellular domain, the potential drops again, probably due to five nearby arginines, namely Arg 274 of the β_2-subunits, Arg 282 of the α_1-subunits, and Arg 304 of the γ_2-subunit.

The interaction profile across the five portals differ. Pathway 1, which runs between an α_1- and a γ_2-subunit, has a deep trough. This is due to the abundance of basic residues on the 'upper' γ_2 intracellular helix that face the portal. They are the Arg 430, Arg 433, Arg 437 and Lys 440. Moreover, there is also Lys 410 on the α_1-subunit. Pathway 2, which runs on the other side of the γ_2 helix, exhibits hardly any energy minimum; the effect of the aforementioned basic residues of the γ_2-subunit is balanced by the acidic residues Asp 442 and Asp 445 on the β_2-subunit. The other three pathways have a moderately low energy minimum, since the intracellular helices generally contain more basic residues than acidic ones.

Fig. 15 shows the structure of the intracellular helices, whose charged amino acids are as follows:

- chain A, β_2-subunit
  - 4× Arg, 3× Lys, 1× His
  - 2× Asp
- chain B, γ_2-subunit
  - 4× Arg, 2× His
  - 2× Asp, 1× Glu
- chain C, α_1-subunit
  - 6× Lys
  - 4× Glu
- chain D, β_2-subunit
  - 4× Arg, 3× Lys, 1× His
  - 2× Asp
- chain E, α_1-subunit
  - 6× Lys
  - 4× Glu

In Fig. 15, the arrows denote the paths taken by the ions whose energy profiles are shown in Fig. 14.

The energy profile has previously been reported for another homology model of the $GABA_A$ receptor [67], where the authors found that the interaction energy decreased as the ion penetrated into the protein, and reached a global minimum near the junction of the extracellular and transmembrane domains. However, the energy increased gradually throughout the transmembrane domain (see Fig. 4 of [67]). The energy profile for a model of the α7 nAChR has also been calculated for the Na^+ ion. The authors reported an energy profile similar to ours (see Fig. 6 of [4]): the energy decreased as the ion entered the protein, then rose in the middle of the extracellular domain, and dropped to a global minimum near the junction of the extracellular and transmembrane domains. The interaction

energy remained high throughout the transmembrane domain, as in our results. Neither report provided data for the intracellular helical parts because they were not modelled. The local energy minimum near the intracellular exit of the ion lends support to the idea that the intracellular helices are partially responsible for ionic selectivity [47].

4. Discussion

There have been a number of attempts to create a model for the $GABA_A$ receptor. The first attempt to model the $GABA_A$ receptor was carried out by Yamakura et al. [100] using low-resolution structural data. O'Mara et al. [67] used the structure of the *L. stagnalis* acetylcholine-binding protein to model the extracellular domain of a $GABA_A$ receptor model, and the structure of the nAChR transmembrane domain to model its transmembrane domain. They used this model for Brownian dynamics simulations. However, it is not certain that such 'glueing' together to form a composite model would create a valid structure.

Ernst et al. [29] produced a model of the $GABA_A$ receptor using the electron microscopy structure of the nAChR [90] (PDB 2BG9). In the present report, we have employed similar methods for comparative modelling, and therefore our alignment and model share many common characteristics with those of [29], including the relative orientation between the extracellular and transmembrane domains, and the packing of the transmembrane helices.

In this work, we have produced two models of the $GABA_A$ receptor. Model 1 is built using the nAChR receptor as a basis (PDB code: 2BG9), while model 2 is built using three AChBPs as bases (PDB codes: 1BJ0, 2BR8 and 1UX2). Comparisons of the two models showed that model 1 is structurally more similar to the apo-form of the receptor, while model 2 is structurally more similar to the liganded form.

4.1. Ligand docking

We have docked two agonists, GABA and muscimol, to the GABA-binding site, together with flunitrazepam and alprazolam to the benzodiazepine-binding site. Different docking methods have different strengths and weaknesses. A comparison of docking programmes [24] used 1000 sample molecules with 49 known ligands, and four methods. The authors concluded that the ability to rank known ligands on the basis of docking results which resemble known crystal structures is both method- and target-dependent. For this reason, we used two different methods in order to explore the docking phase space more thoroughly.

In the application of genetic algorithms [35,40] in molecular docking, the population consists of ligand molecules. The positions, orientations and the conformations of each ligand copy is encoded into the chromosome, as well as the orientations of rotatable hydroxyl groups in the protein. Once the chromosomes are decoded, the internal ligand energy and the interaction energy with the receptor is calculated, and these terms are used to calculate the fitness score. Recombination and mutations are used to create the individuals forming the next generation and as the population is evolved for a specified number of generations, the fitness score gradually increases. Standard parameter configurations were used.

We also apply a recently introduced Quantum Stochastic Tunnelling docking method [44,57,89] as an efficient method for flexible ligand-protein docking to generate multiple docking solutions. This is a hybrid optimization method that combines the advantages of using the potential energy surface (PES) transformation of Stochastic Tunnelling [92] and the multiple coupled-replica search of Path Integral Monte Carlo [32] methods. The energy landscape transformation smooths out the PES and the non-local exploration of the original PES is made possible on the multi-replica PES with increased dimensionality. This combined approach allows for effective tunnelling through high-energy barriers and makes the search for the global energy minimum more efficient.

Approximate scoring functions aim to preserve the native energy landscape in order to correctly identify the native binding mode as the one with the lowest energy. The results of molecular docking simulations suggest that the native binding mode corresponds to a low-energy structure, but not necessarily that with the lowest energy. There is uncertainly in the binding energy values as a consequence of the approximations used. Therefore, the success rate for finding the native binding mode could be significantly increased if the binding mode with the lowest energy is considered together with a small set of distinct binding modes within a certain energy threshold above the lowest-energy binding mode.

It has been found that by selecting a small set of distinct binding mode representatives, the accuracy of the prediction of the experimentally observed binding mode improves substantially [44]. The subsequent rational selection of one or more ligand-binding modes from a list of a few distinct docking poses could be carried out on the basis of a further analysis, as well as on the basis of the known binding mode of other ligands.

4.2. Gating hypothesis

Despite very considerable efforts, the molecular aetiology that underpins the link between agonist recognition and channel activation, remains ill-defined within the cys-loop receptor family. The structural elements that mediate communication between the agonist recognition site, at the subunit interfaces in the extracellular domain, and the M2 helices, the principal components lining the channel pathway through the transmembrane domain, are separated by some 30 Å. However, while it is becoming increasingly clear which structural 'blocks' may be involved in the communication, the side chain interactions within these seem to be rarely conserved across different subgroups of the family [99]. Perhaps this is not surprising, for the gating characteristics of these receptors are complex and distinct, undoubtedly associated with transition states, the nuances of which are only now being explored [82] using the free energy approach introduced by Fersht et al. [31].

These questions have been most fully explored for the nAChR. Agonist binding is obviously the first step in the

process and structural evidence shows that the C-loop caps these binding sites once recognition has occurred [16–18,38]. Comparison of our $GABA_A$ receptor model 1 and model 2 shows that in the capped conformation, the β_2 C-loop becomes closely juxtaposed to the α_1 F-loop. Our analysis of the interatomic distances of residues from model 2 belonging to the F-loop, shows that a stretch of hydrophobic residues, namely Val 208 and Ala 209, near the middle of this loop (Arg Ser Val Val Val Ala Glu Asp), comes as close as 3 Å to the residues at the β-hairpin of the C-loop. Interestingly, the hydrophilic accessibility of these F-loop residues appears to be decreased on exposure of the receptor to the natural agonist [64].

Due to the low level of $GABA_A$ receptor subunit sequence similarity in this region with the AChBPs, and the fact that the F-loop is poorly defined structurally in the cryo-EM nAChR structure, there is no reliable structural template for modelling the F-loop. However, secondary structure analysis of the F-loop using a variety of algorithms indicates a very high propensity of this region for β-strand formation in the $GABA_A$ receptor α_1-subunit. This differs significantly from the F-loops present in AChBPs and 5-HT_3 receptors, which have a higher tendency to random coil and α-helical structure. It is unlikely that the F-loop forms a stable β-strand but it is probably capable of forming transient β-sheet associations with other secondary structural elements of the α_1- or β_2-subunits.

Recent structural reports of recognition between the TonB and TonB-box containing membrane transporters lend some support to such a speculation [68,79]. These studies indicate that the TonB-box, which initially exists as a random coil, undergoes a coil to β-strand transition and packs towards the pre-existing β-sheet of TonB, which serves as a folding template [23]. Indeed the consensus sequence of the TonB-box is surprisingly similar to the sequence observed in the α_1 F-loop, which suggests a similar 'strand invasion' mechanism may occur in the $GABA_A$ receptors. One of the possible partners for transient pairing is the β_2 C-loop that is likely to form a β-hairpin (Val Val Phe Ser Thr). It does not seem unreasonable to suggest that such an interaction may form a communication link between neighboring subunits.

The C-loop leads, via the β10 strand, to the M1 transmembrane helix, and thus is an attractive partner in the communication of the structural changes from the agonist binding site towards the membrane spanning domain. It has been suggested [62] that, in the nAChR, the β10 and β7 strands interact through a salt bridge. Upon agonist occupation, and the consequential C-loop capping of the activation site, a conserved C-loop tyrosine residue is brought into register with the salt-bridge partner from the β7 strand (Lys 139), displacing the salt-bridge partnership between the β10 Asp 194 and β7 Lys 139 that existed in the unoccupied receptor. The equivalent residues in our model of the $GABA_A$ receptor β_2-subunit are quite distinct: the β10 aspartate is replaced by Arg 231, while the salt bridge partner on β7 is Glu 177. The salt-bridge may thus be conserved but there is a charge reversal. However, the tyrosine residue which supplants the interaction with this pair on C-loop closure is replaced in the β_2-subunit of the $GABA_A$ receptor with Lys 220, which may then form an equivalent salt bridge with Glu 177 as the C-loop closes on agonist occupation. It has previously been reported that mutation of Glu 177 leads to spontaneous open channel activity and has been suggested as a trigger for channel gating [65].

Moving to the C-terminal on the β10 sheet, we find an absolutely conserved residue within the family, Arg 240 in this work. It has been suggested that in the nAChR [52], this residue interacts electrostatically with a glutamate residue from loop 2. In our model, this residue, Glu 76, is appropriately placed within 3 Å of the conserved arginine as shown in Fig. 16. It has been proposed that, in the nAChR, the neighbouring valine from this loop (Val77 here), together with the aforementioned glutamate straddle a conserved proline on the M2–M3 linker, also found within the 5-HT_3 receptor where its isomerisation is thought to be responsible for channel gating [55]. The important M2–M3 linker is significantly different within the $GABA_A$ receptor family. The proline residue is replaced, within the $GABA_A$ β_2 sequence, with Lys 303 and the M2–M3 linker is one residue shorter than that found in the nAChRs with the serine residue at the C-terminal end of the M2 helix replaced by Tyr 301 in the $GABA_A$ β_2-subunit. Within the nAChRs this serine residue is important in channel gating [36,82]. As can be seen in Fig. 16, the equivalent Tyr 301 of the $GABA_A$ β_2-subunit is ideally placed to form a hydrogen bond with Asn 78 of loop 2. It is possible that the larger size of Tyr 301 could compensate for the shorter M2–M3 linker length, while preserving the hydrogen bond. We have found that a rotamer and conformation search indicates that this Tyr 301 could also form a hydrogen bond with Glu 76 of loop 2, compatible with a shift of the M2 helix. It is thus possible that this Tyr bonding exchange could play a role of a structural switch as exemplified by the classic example of haemoglobin [69].

As can be seen from Fig. 16, there are a multiplicity of charged residues in this vicinity providing a plethora of potential salt-bridges with additional potential for hydrogen bond formation to the main chain. In view of the continuing

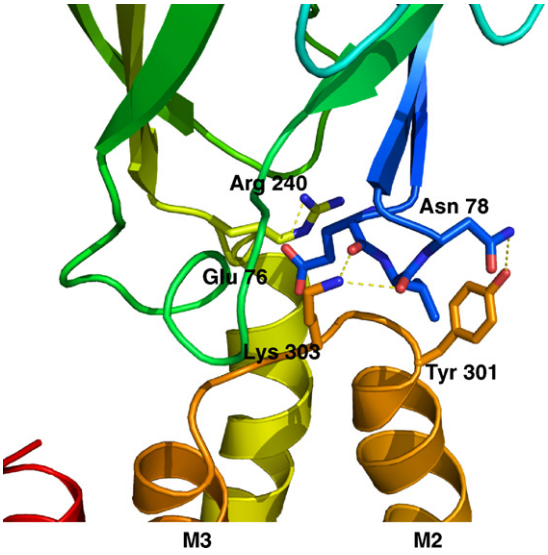

Fig. 16. Diagram showing the region at the junction of the extracellular domain and the transmembrane domain, of the $GABA_A$ receptor β_2-subunit. Putative hydrogen bonds are denoted by dashed lines between the atoms.

analysis of gating schemes within the $GABA_A$ receptor [53], it seems premature to suggest their potential functional roles without the expansion of the experimental work currently available within this arena (see for example [45,59]). It is precisely the purpose of this model building to provide a guide to such experiments, the results of which will allow its further refinement.

Acknowledgements

The authors thank Erika Palin for help with processing data from the Cambridge Structural Database. YM is a recipient of a PhD scholarship from the Algerian Ministry of Higher Education and Scientific Research, MESRS. VNB holds a European Commission Marie Curie Fellowship. This work was partly supported by grants from the Canadian Institutes of Health Research (SMJD and ILM) and the Wellcome Trust (ILM).

References

[1] S.F. Altschul, W. Gish, W. Miller, E.W. Myers, D.J. Lipman, Basic local alignment search tool, J. Mol. Biol. 215 (3) (1990) 403–410.
[2] J. Amin, A. Brooks-Kayal, D.S. Weiss, Two tyrosine residues on the α subunit are crucial for benzodiazepine binding and allosteric modulation of γ-aminobutyric $acid_A$ receptor, Mol. Pharmacol. 51 (1997) 833–841.
[3] J. Amin, D.S. Weiss, $GABA_A$ receptor needs two homologous domains of the β-subunit for activation by GABA but not by pentobarbital, Nature 366 (1993) 565–569.
[4] S. Amiri, K. Tai, O. Beckstein, P.C. Biggin, M.S.P. Sansom, The α7 nicotinic acetylcholine receptor: molecular modelling, electrostatics and energetics, Mol. Membr. Biol. 22 (2005) 151–162.
[5] E.A. Barnard, P. Skolnick, R.W. Olwen, H. Mohler, W. Sieghart, G. Biggio, C. Braestrup, A.N. Bateson, S.Z. Langer, International Union of Pharmacology. XV. Subtypes of γ-aminobutyric $acid_A$ receptors: classification on the basis of subunit structure and receptor function, Pharmacol. Rev. 50 (1998) 291–313.
[6] D.L. Beene, G.S. Brandt, W. Zhong, N.M. Zacharias, H.A. Lester, D.A. Dougherty, Cation-π interactions in ligand recognition by serotonergic ($5\text{-}HT_{3A}$) and nicotinic acetylcholine receptors: the anomalous binding properties of nicotine, Biochemistry 41 (2002) 10262–10269.
[7] D. Berezhnoy, Y. Nyfeler, A. Gonthier, H. Schwob, M. Goeldner, E. Sigel, On the benzodiazepine binding pocket in $GABA_A$ receptors, J. Biol. Chem. 279 (2004) 3160–3168.
[8] J.F. Blount, R.I. Fryer, N.W. Gilman, L.J. Todaro, Quinazolines and 1,4-benzodiazepines. 92. Conformational recognition of the receptor by 1,4-benzodiazepines, Mol. Pharmacol. 24 (1983) 425–428.
[9] A.J. Boileau, A.R. Evers, A.F. Davis, C. Czajkowski, Mapping the agonist binding site of the $GABA_A$ receptor: evidence for a β-strand, J. Neurosci. 19 (1999) 4847–4854.
[10] L. Brehm, K. Frydenvang, L.M. Hansen, P.-O. Norrby, P. Krogsgaard-Larsen, T. Liljefors, Structural features of muscimol, a potent $GABA_A$ receptor agonist. Crystal structure and quantum chemical ab initio calculations, Struct. Chem. 8 (1997) 443–451.
[11] K. Brejc, W.J. van Dijk, R.V. Klaassen, M. Schuurmans, J. van der Oost, A.B. Smit, T.K. Sixma, Crystal structure of an ACh-binding protein reveals the ligand-binding domain of nicotinic receptors, Nature 411 (2001) 269–276.
[12] A. Buhr, R. Baur, E. Sigel, Subtle changes in residue 77 of the γ-subunit of $\alpha_1\beta_2\gamma_2$ $GABA_A$ receptors drastically alter the affinity for ligands of the benzodiazepine binding site, J. Biol. Chem. 272 (1997) 11799–11804.
[13] A. Buhr, M.T. Schaerer, R. Baur, E. Sigel, Residues at positions 206 and 209 of the α_1-subunit of γ-aminobutyric $acid_A$ receptors influence affinities for benzodiazepine binding site ligands, Mol. Pharmacol. 52 (1997) 676–682.
[14] A. Buhr, E. Sigel, A point mutation in the γ_2-subunit of the γ-aminobutyric acid type A receptors result in altered benzodiazepine binding specificity, Proc. Natl. Acad. Sci. USA 94 (1997) 8824–8829.
[15] H. Butcher, T.A. Hamor, I.L. Martin, Structures of 7-bromo-1,3-dihydro-5-(2-pyridyl)-2*H*-1,4-benzodiazepin-2-one (bromazepam, $C_{14}H_{10}BrN_3O$) and 5-(2-fluorophenyl)-1,3-dihydro-1-methyl-7-nitro-2*H*-1,4-benzodiazepin-2-one (flunitrazepam, $C_{16}H_{12}FN_3O_3$), Acta Crystallogr. C39 (1983) 1469–1472.
[16] P.H.N. Celie, I.E. Kasheverov, D.Y. Mordvintsev, R.C. Hogg, P. van Nierop, R. van Elk, S.E. van Rossum-Fikkert, M.N. Zhmak, D. Bertrand, V. Tsetlin, T.K. Sixma, A.B. Smit, Crystal structure of nicotinic acetylcholine receptor homolog AChBP in complex with an alpha-conotoxin PnIA variant, Nat. Struct. Mol. Biol. 12 (2005) 582–588.
[17] P.H.N. Celie, R.V. Klaassen, S.E. van Rossum-Fikkert, R. van Elk, P. van Nierop, A.B. Smit, T.K. Sixma, Structure of acetylcholine-binding protein from *Bulinus truncatus* reveals the conserved structural scaffold and sites of variation in nicotinic acetylcholine receptors, J. Biol. Chem. 280 (2005) 26457–26466.
[18] P.H.N. Celie, S.E. van Rossum-Fikkert, W.J. van Dijk, K. Brejc, T.K. Sixma, A.B. Smit, Nicotine and carbamylcholine binding to nicotinic acetylcholine receptors as studied in AChBP crystal structures, Neuron 41 (2004) 907–914.
[19] P.-L. Chau, P.M. Dean, Molecular recognition: 3D surface structure comparison by gnomonic projection, J. Mol. Graph. 5 (1987) 97–100.
[20] P.-L. Chau, P.M. Dean, Electrostatic complementarity between proteins and ligands. 1. Charge disposition, dielectric and interface effects, J. Comput-Aided Mol. Des. 8 (1994) 513–525.
[21] P.-L. Chau, P.M. Dean, Electrostatic complementarity between proteins and ligands. 2. Ligand moieties, J. Comput.-Aided Mol. Des. 8 (1994) 527–544.
[22] P.-L. Chau, P.M. Dean, Electrostatic complementarity between proteins and ligands. 3. Structural basis, J. Comput.-Aided Mol. Des. 8 (1994) 545–564.
[23] D.P. Chimento, A.K. Mohanty, R.J. Kadner, M.C. Wiener, Substrate-induced transmembrane signaling in the cobalamin transporter BtuB, Nat. Struct. Biol. 10 (2003) 394–401.
[24] M.D. Cummings, R.L. DesJarlais, A.C. Gibbs, V. Mohan, E.P. Jaeger, Comparison of automated docking programs as virtual screening tools, J. Med. Chem. 48 (2005) 962–976.
[25] P.M. Dean, P.-L. Chau, M.T. Barakat, Development of quantitative methods for studying electrostatic complementarity in molecular recognition and drug design, J. Mol. Struct. (THEOCHEM) 256 (1992) 75–89.
[26] J.M.C. Derry, I.M. Paulsen, M. Davies, S.M.J. Dunn, A single point mutation of the $GABA_A$ receptor α5 subunit confers fluoxetine sensitivity, Neuropharmacology 52 (2007) 497–505.
[27] L.L. Duncalfe, M.R. Carpenter, L.B. Smillie, I.L. Martin, S.M.J. Dunn, The major site of photoaffinity labeling of the γ-aminobutyric acid type A receptor by [^{3}H]-flunitrazepam is histidine 120 of the α subunit, J. Biol. Chem. 271 (1996) 9209–9214.
[28] S.M.J. Dunn, M. Davies, A.L. Muntoni, J.J. Lambert, Mutagenesis of the rat α1 subunit of the γ-aminobutyric $acid_A$ receptor reveals the importance of residue 101 in determining the allosteric effects of benzodiazepine site lingads, Mol. Pharmacol. 56 (1999) 768–774.
[29] M. Ernst, S. Bruckner, S. Boresch, W. Sieghart, Comparative models of $GABA_A$ receptor extracellular and transmembrane domains: important insights in pharmacology and function, Mol. Pharmacol. 68 (2005) 1291–1300.
[30] S.J. Farrar, P.J. Whiting, T.P. Bonnert, R.M. McKernan, Stoichiometry of a ligand-gated ion channel determined by fluorescence energy transfer, J. Biol. Chem. 274 (1999) 10100–10104.
[31] A.R. Fersht, R.J. Leatherbarrow, T.N.C. Wells, Quantitative analysis of structure–activity relationships in engineered proteins by linear free-energy relationships, Nature 322 (1986) 284–286.
[32] R.P. Feynman, A.R. Hibbs, Quantum Mechanics and Path Integrals, McGraw-Hill, New York, 1965.

[33] A. Fiser, R.K. Do, A. Sali, Modeling of loops in protein structures, Protein Sci. 9 (9) (2000) 1753–1773.
[34] R.I. Fryer, Ligand interactions at the benzodiazepine receptor, in: C. Hansch, P. Sammes, J. Taylor (Eds.), J.C. Emmett ed., Comprehensive Medicinal Chemistry, vol. 3, Pergammon Press, Oxford, 1990, pp. 539–566.
[35] D.E. Goldberg, Genetic Algorithms in Search, Optimization and Machine Learning, Addison-Wesley, Reading, Massachusetts, 1989.
[36] C. Grosman, F.N. Salamone, S.M. Sine, A. Auerbach, The extracellular linker of muscle acetylcholine receptor is a gating control element, J. Gen. Physiol. 116 (2000) 327–340.
[37] T.G. Hales, J.I. Dunlop, T.Z. Deeb, J.E. Carland, S.P. Kelley, J.J. Lambert, J.A. Peters, Common determinants of single channel conductance within the large cytoplasmic loop of 5-HT_3 and $\alpha4\beta2$ nicotinic acetylcholine receptors, J. Biol. Chem. 281 (2006) 8062–8071.
[38] S.B. Hansen, G. Sulzenbacher, T. Huxford, P. Marchot, P. Taylor, Y. Bourne, Structures of *Aplysia* AChBP complexes with nicotinic agonists and antagonists reveal distinctive binding interfaces and conformations, EMBO J. 24 (2005) 3635–3646.
[39] H.C. Hemmings, M.H. Akabas, P.A. Goldstein, J.R. Trudell, B.A. Orser, N.L. Harrison, Emerging molecular mechanisms of general anesthetic action, Trends Pharmacol. Sci. 26 (2005) 503–510.
[40] J.H. Holland, Adaptation in Natural and Artificial System, University of Michigan Press, Ann Arbor, Michigan, 1975.
[41] A. Jenkins, E.P. Greenblatt, H.J. Faulkner, E. Bertaccini, A. Light, A. Lin, A. Andreasen, A. Viner, J.R. Trudell, N.L. Harrison, Evidence for a common binding cavity for three general anesthetics within the $GABA_A$ receptor, J. Neurosci. 21 (2001) RC136–RC139.
[42] G. Jones, P. Willet, R.C. Glen, Molecular recognition of receptor sites using a genetic algorithm with a description of desolvation, J. Mol. Biol. 245 (1995) 43–53.
[43] G. Jones, P. Willet, R.C. Glen, A.R. Leach, R. Taylor, Development and validation of a genetic algorithm for flexible docking, J. Mol. Biol. 267 (1997) 727–748.
[44] P. Källblad, R.L. Mancera, N.P. Todorov, Assessment of multiple binding modes in ligand-protein docking, J. Med. Chem. 47 (2004) 3334–3337.
[45] T.L. Kash, J.R. Trudell, N.L. Harrison, Structural elements involved in activation of the γ-aminobutyric acid type A ($GABA_A$) receptor, Biochem. Soc. Trans. 32 (2004) 540–546.
[46] K. Katoh, K. Kuma, H. Toh, T. Miyata, MAFFT version 5: improvement in accuracy of multiple sequence alignment, Nucl. Acids Res. 33 (2) (2005) 511–518.
[47] S.P. Kelley, J.I. Dunlop, E.F. Kirkness, J.J. Lambert, J.A. Peters, A cytoplasmic region determines single-channel conductance in 5-HT_3 receptors, Nature 424 (2003) 321–324.
[48] G. Klebe, Virtual ligand screening: strategies, perspectives and limitations, Drug Discov. Today 11 (2006) 580–594.
[49] A. Krogh, B. Larsson, G. von Heijne, E.L. Sonnhammer, Predicting transmembrane protein topology with a hidden Markov model: application to complete genomes, J. Mol. Biol. 305 (3) (2001) 567–580.
[50] A.M. Kucken, J.A. Teissére, J. Seffinga-Clark, D.A. Wagner, C. Czajkowski, Structural requirements for imidazobenzodiazepine binding to $GABA_A$ receptors, Mol. Pharmacol. 63 (2003) 289–296.
[51] A.M. Kucken, D.A. Wagner, P.R. Ward, J.A. Teissére, A.J. Boileau, C. Czajkowski, Identification of benzodiazepine binding site residues in the γ_2-subunit of the γ-aminobutyric acid A receptor, Mol. Pharmacol. 57 (2000) 932–939.
[52] W.Y. Lee, S.M. Sine, Principal pathway coupling agonist to channel gating in nicotinic receptors, Nature 438 (2005) 243–247.
[53] G.M.C. Lema, A. Auerbach, Modes and models of $GABA_A$ receptor gating, J. Physiol. 572 (2006) 183–200.
[54] S.C.R. Lummis, D.L. Beene, N.J. Harrison, H.A. Lester, D.A. Dougherty, A cation-π binding interaction with a tyrosine in the binding site of the $GABA_C$ receptor, Chem. Biol. 12 (2005) 993–997.
[55] S.C.R. Lummis, D.L. Beene, L.W. Lee, H.A. Lester, R.W. Broadhurst, D.A. Dougherty, *Cis–trans* isomerization at a proline opens the pore of a neurotransmitter-gated ion channel, Nature 438 (2005) 248–252.
[56] R. Luthy, J.U. Bowie, D. Eisenberg, Assessment of protein models with three-dimensional profiles, Nature 356 (6364) (1992) 83–85.
[57] R.L. Mancera, P. Källblad, N.P. Todorov, Ligand-protein docking using a quantum stochastic tunneling optimization method, J. Comput. Chem. 25 (2004) 858–864.
[58] Chemical Computing Group Inc., MOE (Molecular Operating Environment) Version 2005.06, Chemical Computing Group Inc., Montreal, Canada, 2005.
[59] J. Mercado, C. Czajkowski, Charged residues in the α_1 and β_2 pre-M1 regions involved in $GABA_A$ receptor activation, J. Neurosci. 26 (2006) 2031–2040.
[60] A. Miyazawa, Y. Fujiyoshi, N. Unwin, Structure and gating mechanism of the acetylcholine receptor pore, Nature 423 (2003) 949–955.
[61] K. Mizuguchi, C.M. Deane, T.L. Blundell, M.S. Johnson, J.P. Overington, JOY: protein sequence-structure representation and analysis, Bioinformatics 14 (7) (1998) 617–623.
[62] N. Mukhtasimova, C. Free, S.M. Sine, Initial coupling of binding to gating mediated by conserved residues in the muscle nicotinic receptor, J. Gen. Physiol. 126 (1998) 23–39.
[63] N. Nayeem, T.P. Green, I.L. Martin, E.A. Barnard, Quaternary structure of the native $GABA_A$ receptor determined by electron microscopic image analysis, J. Neurochem. 62 (1994) 815–818.
[64] J.G. Newell, C. Czajkowski, The $GABA_A$ receptor α1 subunit Pro174–Asp 191 segment is involved in GABA binding and channel gating, J. Biol. Chem. 278 (2003) 13166–13172.
[65] J.G. Newell, R.A. McDevitt, C. Czajkowski, Mutation of glutamate 155 of the $GABA_A$ receptor β_2 subunit produces a spontaneously open channel: a trigger for channel activation, J. Neurosci. 24 (2004) 11226–11235.
[66] J.W. Nissink, C. Murray, M. Hartshorn, M.L. Verdonk, J.C. Cole, R. Taylor, A new test set for validating predictions of protein-ligand interaction, Proteins 49 (2002) 457–471.
[67] M. O'Mara, B. Cromer, M. Parker, S.-H. Chung, Homology model of the $GABA_A$ receptor examined using Brownian dynamics, Biophys. J. 88 (2005) 3286–3299.
[68] P.D. Pawelek, N. Croteau, C. Ng-Thow-Hing, C.M. Khursigara, N. Moiseeva, M. Allaire, J.W. Coulton, Structure of TonB in complex with FhuA, *E. coli* out membrane receptor, Science 312 (2006) 1399–1402.
[69] M.F. Perutz, A.J. Wilkinson, M. Paoli, G.G. Dodson, The stereo-chemical mechanism of the cooperative effects in hemoglobin revisited, Annu. Rev. Biophys. Biomol. Struct. 27 (1998) 1–34.
[70] S. Pirker, C. Schwarzer, A. Wieselthaler, W. Sieghart, G. Sperk, $GABA_A$ receptors: immunocytochemical distribution of 13 subunits in the adult rat brain, Neuroscience 101 (2000) 815–850.
[71] J.W. Ponder, D.A. Case, Force fields for protein simulations, Adv. Protein Chem. 66 (2003) 27–85.
[72] G. Reck, W. Thiel, F. Bahr, W. Sauer, D. Scharfenberg-Pfeiffer, K.-F. Landgraf, X-ray investigations on three crystalline forms of alprazolam (in German), Pharmazie 51 (1996) 553–557.
[73] R.B. Russell, G.J. Barton, Multiple protein sequence alignment from tertiary structure comparison: assignment of global and residue confidence levels, Proteins 14 (2) (1992) 309–323.
[74] A. Sali, T.L. Blundell, Definition of general topological equivalence in protein structures. A procedure involving comparison of properties and relationships through simulated annealing and dynamic programming, J. Mol. Biol. 212 (2) (1990) 403–428.
[75] A. Sali, T.L. Blundell, Comparative protein modelling by satisfaction of spatial restraints, J. Mol. Biol. 234 (3) (1993) 779–815.
[76] M.T. Schaerer, A. Buhr, R. Baur, E. Sigel, Amino acid 200 on the α_1-subunit of $GABA_A$ receptors affect the interaction with selected benzodiazepine binding site ligands, Eur. J. Pharmacol. 354 (1998) 283–287.
[77] D. Scharf, K. Laasonen, Structure, effective pair potential and properties of halothane, Chem. Phys. Lett. 258 (1996) 276–282.
[78] J. Shi, T.L. Blundell, K. Mizuguchi, FUGUE: sequence-structure homology recognition using environment-specific substitution tables and structure-dependent gap penalties, J. Mol. Biol. 310 (1) (2001) 243–257.
[79] D.D. Shultis, M.D. Purdy, C.N. Banchs, M.C. Wiener, Outer membrane active transport: structure of the BtuB:TonB complex, Science 312 (2006) 1396–1399.

[80] N. Siew, A. Elofsson, L. Rychlewski, D. Fischer, MaxSub: an automated measure for the assessment of protein structure prediction quality, Bioinformatics 16 (2000) 776–785.
[81] E. Sigel, R. Baur, S. Kellenberger, P. Malherbe, Point mutations affecting antagonist affinity and agonist dependent gating of $GABA_A$ receptor channels, EMBO J. 11 (1992) 2017–2023.
[82] S.M. Sine, A.G. Engel, Recent advances in Cys-loop receptor structure and function, Nature 440 (2006) 448–455.
[83] G.B. Smith, R.W. Olsen, Identification of a [^{3}H]-muscimol photoaffinity substrate in the bovine γ-aminobutyric acid A receptor α-subunit, J. Biol. Chem. 269 (1994) 20380–20387.
[84] G.B. Smith, R.W. Olsen, Deduction of the amino acid residues in the $GABA_A$ receptor α-subunits photoaffinity labeled with the benzodiazepine flunitrazepam, Neuropharmacology 39 (2000) 55–64.
[85] C.E. Spearman, 'General intelligence' objectively determined and measured, Am. J. Psychol. 15 (1904) 201–293.
[86] C.E. Spearman, Proof and measurement of association between two things, Am. J. Psychol. 15 (1904) 72–101.
[87] T. Steinmetzer, M. Renatus, S. Künzel, A. Eichinger, W. Bode, P. Wikström, J. Hauptmann, J. Stürzebecher, Design and evaluation of novel bivalent thrombin inhibitors based on amidinophenylalanines, Eur. J. Biochem. 265 (1999) 598–605.
[88] W.R. Taylor, The classification of amino acid conservation, J. Theor. Biol. 119 (1986) 205–218.
[89] N.P. Todorov, R.L. Mancera, P.H. Monthoux, A new quantum stochastic tunneling optimisation method for protein-ligand, Chem. Phys. Lett. 369 (2003) 257–263.
[90] N. Unwin, Refined structure of the nicotinic acetylcholine receptor at 4 Å resolution, J. Mol. Biol. 346 (4) (2005) 967–989.
[91] D.A. Wagner, C. Czajkowski, Structure and dynamics of the GABA binding pocket: a narrowing cleft that constricts during activation, J. Neurosci. 21 (2001) 67–74.
[92] W. Wenzel, K. Hamacher, Stochastic tunneling approach for global minimization of complex potential energy landscapes, Phys. Rev. Lett. 82 (1999) 3003–3007.
[93] S.E. Westh-Hansen, P.B. Rasmussen, S. Hastrup, J. Nabekura, K. Noguchi, N. Akaike, M.-R. Witt, M. Nielsen, Decreased agonist sensitivity of human $GABA_A$ receptors by an amino acid variant, isoleucine to valine, in the α_1-subunit, Eur. J. Pharmacol. 329 (1997) 253–257.
[94] S.E. Westh-Hansen, M.-R. Witt, K. Dekermendjian, T. Liljefors, P.B. Rasmussen, M. Nielsen, Arginine residue 120 of the human $GABA_A$ receptor α_1-subunit is essential for GABA binding and chloride ion current gating, Neuroreport 10 (1999) 2417–2421.
[95] P.J. Whiting, $GABA_A$ receptor subtypes in the brain: a paradigm for CNS drug discovery? Drug Discov. Today 8 (2003) 445–450.
[96] H.A. Wieland, H. Lüddens, P.H. Seeburg, A single histidine in $GABA_A$ receptors is essential for benzodiazepine binding, J. Biol. Chem. 267 (1992) 1426–1429.
[97] P.B. Wingrove, S.A. Thompson, K.A. Wafford, P.J. Whiting, Key amino acids in the γ-subunit of the γ-aminobutyric $acid_A$ receptor that determine ligand binding and modulation at the benzodiazepine binding site, Mol. Pharmacol. 52 (1997) 874–881.
[98] C.H. Wu, R. Apweiler, A. Bairoch, D.A. Natale, W.C. Barker, B. Boeckmann, S. Ferro, E. Gasteiger, H. Huang, R. Lopez, M. Magrane, M.J. Martin, R. Mazumder, C. O'Donovan, N. Redaschi, B. Suzek, The Universal Protein Resource (UniProt): an expanding universe of protein information, Nucl. Acids Res. 34 (Database issue) (2006) D187–D191.
[99] X. Xiu, A.P. Hanek, J. Wang, H.A. Lseter, D.A. Dougherty, A unified view of the role of electrostatic interactions in modulating the gating of the Cys loop receptors, J. Biol. Chem. 280 (2005) 41655–41666.
[100] T. Yamakura, E. Bertaccini, J.R. Trudell, R.A. Harris, Anaesthetics and ion channels: molecular models and sites of action, Annu. Rev. Pharmacol. Toxicol. 41 (2001) 23–51.